Size-dependent electric voltage controlled magnetic anisotropy in multiferroic heterostructures: Interface-charge and strain comediated magnetoelectric coupling

Jia-Mian Hu,[1,2] Ce-Wen Nan,[1,*] and Long-Qing Chen[2]

[1]*Department of Materials Science and Engineering, and State Key Lab of New Ceramics and Fine Processing, Tsinghua University, Beijing 100084, China*

[2]*Department of Materials Science and Engineering, Pennsylvania State University, University Park, Pennsylvania 16802-5005, USA*

(Received 21 November 2010; revised manuscript received 10 January 2011; published 8 April 2011)

We present a phenomenological scheme to study the size-dependent electric voltage-controlled magnetic anisotropy in ferromagnetic (FM) and ferroelectric (FE) heterostructures. The FM layers are either metallic [Fe(001), Ni(001), Co(0001)] or half-metallic [(La, Sr)MnO_3] films. Two magnetoelectric mechanisms, i.e., interface-charge and strain-mediated couplings, are considered. We show that the interface-charge-mediated coupling is the main mechanism for the magnetoelectic coupling when the FM film thickness is below a certain transition thickness d_{tr} while the strain-mediated coupling dominates above d_{tr}.

DOI: 10.1103/PhysRevB.83.134408 PACS number(s): 75.80.+q, 75.70.Cn, 75.30.Gw

I. INTRODUCTION

Artificial multiferroic heterostructures of ferroelectric (FE) and ferromagnetic (FM) layers are of increasing interest due to the coupling between the magnetic and electric polarizations.[1–3] Of particular interest in the multiferroic heterostructures, electric voltage, rather than the usual current or magnetic field, can be directly used to control the magnetic anisotropy or magnetization direction via magnetoelectric (ME) coupling,[1–5] which offers promising applications for novel spintronic or ME devices with much lower power consumption and higher speed. Examples include voltage-driven magnetic random access memories,[6–8] logic circuits,[9] and microwave devices.[10,11] Much effort has been devoted to achieve robust *room-temperature* ME coupling by virtue of such FE/FM heterostructures through a strain-induced ME effect across an interface,[4,12–18] an interface-charges-driven ME effect,[19–23] or magnetic exchange bias.[24–29] As demonstrated recently in the multiferroic heterostructures, a remarkable electric-voltage control of magnetic behavior of the magnetic nanostructures at *room temperature* can be achieved by a strain-induced ME coupling, i.e., an external voltage in the ferroelectric layer causing a strain change across the interface and then altering the magnetic anisotropy of the magnetic layer via magnetoelastic coupling. For example, a butterfly-shaped magnetization-electric field (*M-E*) loop at room temperature has recently been observed in a multiferroic FM/FE heterostructure with a $La_{0.7}Sr_{0.3}MnO_3$ (LSMO, 20–50 nm) thin film grown on $Pb(Mg_{1/3}Nb_{2/3})_{0.72}Ti_{0.28}O_3$ (PMN-PT), which tracks the butterfly-shaped strain-*E* loop of PMN-PT, demonstrating a strain-induced ME coupling across the LSMO/PMN-PT interface.[12] However, in a multiferroic $PbZr_{0.2}Ti_{0.8}O_3$ (PZT, 250 nm)/LSMO (4 nm)/$SrTiO_3$ (001) heterostructure,[19] a totally different square-shaped *M-E* hysteric loop has been observed at 100 K. Although a larger piezostrain could be expected in such a reverse FE/FM/substrate structure, further tests using x-ray absorption near edge spectroscopy[20] explicitly illustrated an interface-charge-driven ME coupling, i.e., a direct voltage-induced modification of the magnetocrystalline anisotropy through a change in interfacial spin configuration.[21–23] This discrepancy thus raises important questions: Why do the two heterostructures behave differently, or do these two different ME coupling mechanisms operate independently? In this work, we demonstrate these coupling mechanisms could coexist and tend to interact with each other at the interfaces. Specifically, the interface-charge-mediated ME coupling exerts major influences for ultrathin FM films while the strain-mediated ME coupling operates at larger thickness, leading to a size dependent electric-voltage control of magnetic anisotropy.

In this article we present a phenomenological approach to investigate such size effect of the ME coupling in the multiferroic FM/FE heterostructure, where the influences of two mechanisms for the ME coupling, i.e., the interface-charge- and strain-mediated coupling, are addressed. For illustration, we consider different FM films, including either metallic [Fe(001), Ni(001), Co(0001)] or half-metallic (001)-oriented LSMO films, grown on an FE layer such as $BaTiO_3$(001). The results show that there is a transition thickness d_{tr} for the FM films, i.e., in the FM/FE heterostructures with a thin FM film below d_{tr}, the interface-charge-mediated coupling plays a major part, while the strain-mediated ME coupling predominates when the FM film thickness is larger than d_{tr}.

II. PHENOMENOLOGICAL MODEL

Consider a multiferroic structure with a FM thin film grown on a FE layer and an electric voltage V applied longitudinally across the FE layer. Then the total magnetic anisotropy energy $F_{tot}(V)$ of the FM film in a single-domain state is[7,8,18]

$$F_{tot}(V) = F_{mc} + F_{shape} + F_{me}(V) + F_S(V), \tag{1}$$

where F_{mc} is the magnetocrystalline anisotropy, F_{shape} the shape anisotropy, F_{me} the magnetoelastic anisotropy, and F_S the surface anisotropy, The strain-induced coupling across the interface and the interface-charge driven coupling are mainly related to the magnetoelastic anisotropy F_{me} and the surface anisotropy F_S, respectively, where F_S can be expressed as[22,30]

$$F_{surf} = -\frac{2K_s + \Delta K_s(V)}{d} m_3^2, \tag{2}$$

where m_3 refers to the direction cosine, K_s and $\Delta K_s(V)$ denote the surface anisotropy energy and its change under external

electric voltage V, and d is the thickness of the FM film. Any changes in the interface charges would alter the surface anisotropy and hence the magnetization state.

For simplicity, the effective magnetic anisotropy field H_{eff}[10,11,31] is used to investigate the voltage-controlled magnetic anisotropy (H_{eff} usually shares a similar variation trend with the magnetic coercive field H_c[32]). Thus the out-of-plane effective anisotropy field, i.e., $H_{\text{eff}}^{\text{OP}}$, can be determined by

$$H_{\text{eff}}^{\text{OP}} = -\frac{1}{\mu_0 M_s}\frac{\partial F_{\text{tot}}}{\partial m_3}\bigg|_{m_3=1}, \tag{3}$$

where μ_0 and M_s are the vacuum permeability and the saturation magnetization, respectively. Combination of Eq. (3) with Eq. (1) yields under zero voltage bias

$$H_{\text{eff}}^{\text{OP}} = \frac{2K_1}{M_s} - \mu_0 M_s + \frac{2\left[B_1\left(1+\frac{2c_{12}}{c_{11}}\right)\varepsilon_0\right]}{M_s} + \frac{4K_s}{dM_s} \tag{4a}$$

for cubic (001)-oriented FM films and

$$H_{\text{eff}}^{\text{OP}} = \frac{2K_1}{M_s} - \mu_0 M_s - \frac{2B_4^2}{c_{44}M_s} + \frac{2\left(B_1+2B_3-\frac{2B_2c_{13}}{c_{33}}\right)\varepsilon_0}{M_s} + \frac{4K_s}{dM_s} \tag{4b}$$

for hexagonal (0001) films. K_1 and B_i (i = 1,2,3,4) denote the magnetocrystalline and magnetoelastic constants, respectively; c_{ij} and ε_0 are the elastic stiffness constants and the residual strain in the FM films, respectively. $H_{\text{eff}}^{\text{OP}}$ can be experimentally obtained from an out-of-plane magnetic hysteresis loop.[33] An out-of-plane magnetic easy axis (or spontaneous magnetization) is preferred for $H_{\text{eff}}^{\text{OP}} > 0$, and a change in the sign of $H_{\text{eff}}^{\text{OP}}$ from positive to negative would indicate an easy axis reorientation[18] from an out-of-plane to an in-plane direction or vice versa. Such a reorientation depending on the film thickness has been reported in FM thin films.[30,34,35] For example, in a Ni/Cu(001) heterostructure,[34] the easy axis of the magnetization switched abruptly from initial in-plane to out-of-plane at a critical thickness d_{cr} of about 10.5 monolayers (ML) (i.e., ~1.6 nm). The critical thickness d_{cr} for such an easy axis reorientation can be estimated from $H_{\text{eff}}^{\text{OP}} = 0$, i.e., $d_{\text{cr}} = 2K_s/[\frac{1}{2}\mu_0 M_s^2 - K_1 - B_1(1+2c_{12}/c_{11})\varepsilon_0]$. By using the known material parameters,[36] and the residual strain ε_0 of 2.5% arising from the in-plane lattice mismatch between the Ni film and Cu(001) substrate,[34] one can obtain d_{cr} of about 1.73 nm for the Ni film, well consistent with the experimental value (~1.6 nm), demonstrating that this effective anisotropy field approach is valid.

Now let us return to the change in the magnetic anisotropy under the application of longitudinal electric voltages to the bilayer structure, i.e., $\Delta H_{\text{eff}}^{\text{OP}}$ [$= H_{\text{eff}}^{\text{OP}}(V)/H_{\text{eff}}^{\text{OP}}(0) - 1$], which can be obtained as

$$\Delta H_{\text{eff}}^{\text{OP}} = \frac{2\left[B_1\left(1+\frac{2c_{12}}{c_{11}}\right)\varepsilon_p(V) + \frac{\Delta K_s(V)}{d}\right]}{M_s} \Big/ H_{\text{eff}}^{\text{OP}} \tag{5a}$$

for cubic (001) FM films and

$$\Delta H_{\text{eff}}^{\text{OP}} = \frac{2\left[\left(B_1+2B_3-\frac{2B_2c_{13}}{c_{33}}\right)\varepsilon_p(V) + \frac{\Delta K_s(V)}{d}\right]}{M_s} \Big/ H_{\text{eff}}^{\text{OP}} \tag{5b}$$

for hexagonal (0001) films. $\varepsilon_p(V)$ denotes the piezostrain under external voltage. The two terms in the square brackets on the right-hand side of Eq. (5) describe the contributions from the strain- and the interface-charge-mediated ME coupling. Thus these two mechanisms coexist in the FM/FE bilayer structure and compete with each other.

III. RESULTS AND DISCUSSION

For illustration, the calculations are performed for the FM films by using the known material parameters,[36] and a common $BaTiO_3$ (BTO) film with a thickness of about 100 nm grown on a (001) $SrTiO_3$ substrate[41] is chosen as the FE layer, with $SrRuO_3$ as a bottom electrode. The butterfly-shaped curve of piezostrain $\varepsilon_p(V)$ shown in Fig. 1(a) v was measured in the BTO film using a piezoelectric force microscope. For the metallic Fe(001) films, the hysteresis-like change in $\Delta K_s(V)$ [Fig. 1(b)] is directly assumed from the experimental measurements of voltage-controlled magnetic anisotropy in ultrathin Fe atomic layers.[22] However, no results on the voltage-induced magnetic anisotropy are now available

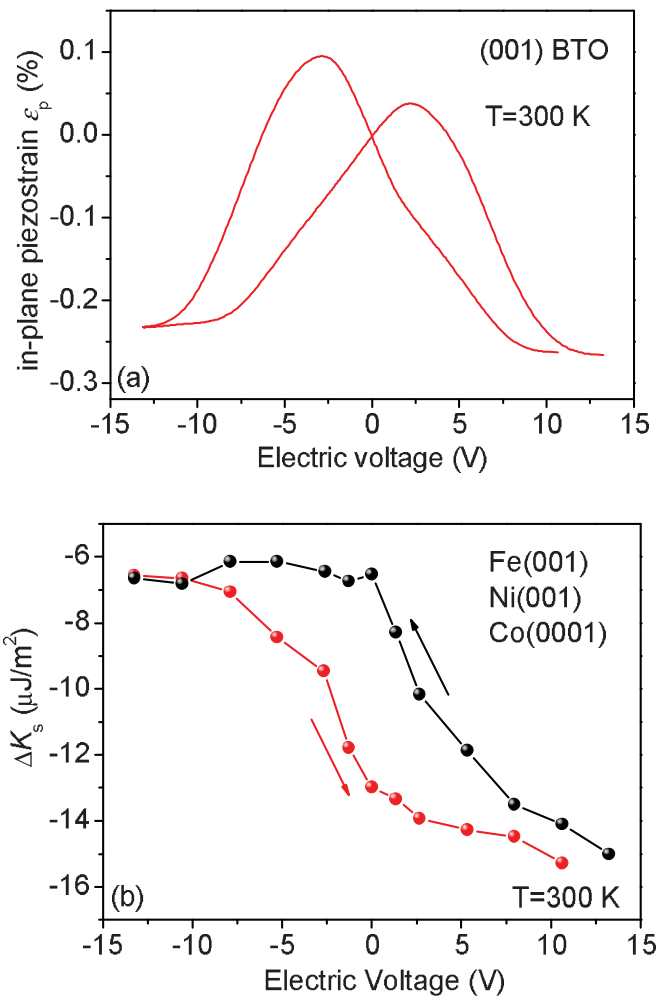

FIG. 1. Electric voltage dependence of (a) the in-plane piezostrain ε_p generated in the (001) $BaTiO_3$ (BTO) film and (b) the surface anisotropy energy change ΔK_s in the Fe(001), Ni(001) and Co(0001) films.

for the metallic Ni(001) and Co(0001) films. For the sake of simplicity, the same $\Delta K_s(V)$ is tentatively used for the Ni(001) and Co(0001) films herein, although $\Delta K_s(V)$ could differ in these three transition-metal films and support from both experiments and *ab initio* calculations are awaited. Actually, recent density functional calculations[42] showed that ultrathin Ni and Co films exhibited quite similar voltage-induced surface ME coefficients to Fe, i.e., 2.9×10^{-14} G cm^2/V for a 15-ML Fe(001) film with perpendicular [001] magnetization, 3.0×10^{-14} G cm^2/V for 9-ML Ni(001) with in-plane [100] magnetization, and 1.7×10^{-14} G cm^2/V for 9-ML Co(0001) film with [001] magnetization.

As the first example, the electric voltage-induced changes in $H_{\rm eff}^{\rm OP}$ for the (001) Fe/BTO thin-film heterostructure are shown in Fig. 2(a). It shows distinct size-dependent characteristics of the voltage-controlled out-of-plane effective anisotropy field, i.e., $\Delta H_{\rm eff}^{\rm OP}$, demonstrating the coexistence of both the interface-charge- and strain-mediated ME coupling in the heterostructure. A transition thickness $d_{\rm tr}$ for the two interacting ME coupling mechanisms can be estimated to be about 0.5 nm (about one-unit cell thickness) as the contributions from the two mechanisms become equal from Eq. (5). Thus, when the Fe film thickness is smaller than $d_{\rm tr}$ (e.g., 0.2 nm), the $\Delta H_{\rm eff}^{\rm OP}$-voltage curve tends to mimic the voltage-induced surface anisotropy change behavior, i.e., a hysteresis-like loop [see Fig. 2(a)], indicating that the interface-charge-mediated ME coupling could play a major part. However, the $\Delta H_{\rm eff}^{\rm OP}$-voltage loops become butterfly-shaped as the film thickness exceeds $d_{\rm tr}$, presenting a dominant strain-mediated ME effect. An external voltage leads to larger changes in $\Delta H_{\rm eff}^{\rm OP}$ in Fe films with smaller thickness (i.e., below $d_{\rm tr}$), as compared to those with thickness larger than $d_{\rm tr}$. Such larger $\Delta H_{\rm eff}^{\rm OP}$ can in principle allow a more dramatic voltage-induced magnetic anisotropy change based on a dominative interface-charge ME coupling in the reduced thickness scale. Moreover, the maximal value of $\Delta H_{\rm eff}^{\rm OP}$ emerges at $d = 0.3$ nm to be about 20% under the action of negative voltages, which could be attributed to the enhanced sensitivity of $\Delta H_{\rm eff}^{\rm OP}$ to both the external voltage and the residual strain when approaching the transition thickness $d_{\rm tr}$, as illustrated in Fig. 2(b). Furthermore, it can be seen that the $\Delta H_{\rm eff}^{\rm OP}$-voltage loop reverses as the film thickness increases from 0.3 to 1 nm, due to a sign change of $H_{\rm eff}^{\rm OP}$ at a critical thickness $d_{\rm cr}$ of about 0.39 nm (not shown here) where the magnetic easy axis of the Fe film switches from an out-of-plane to an in-plane direction.

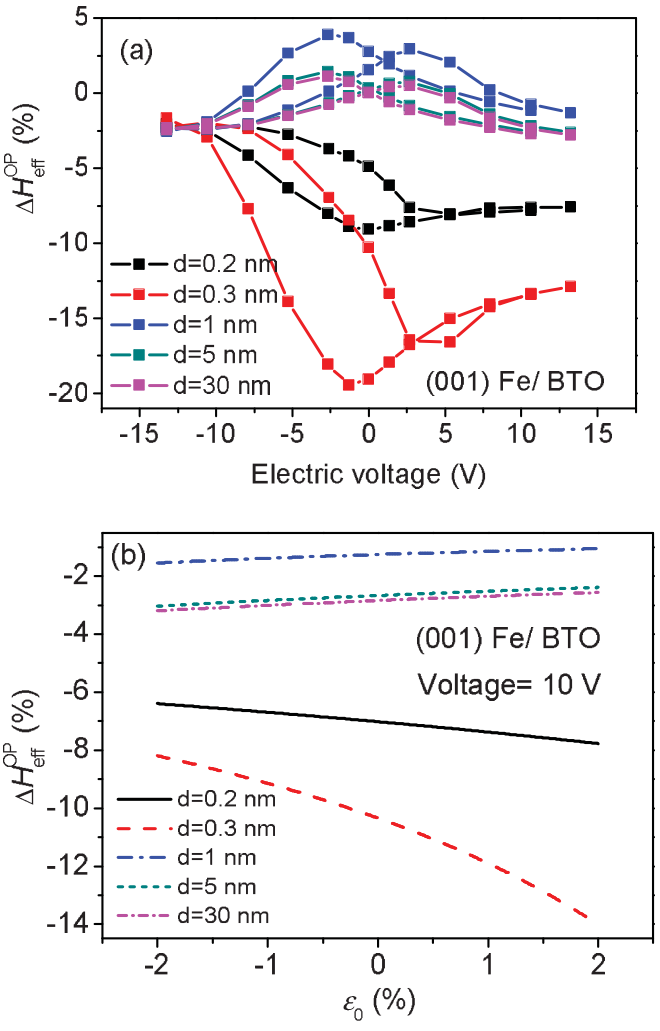

FIG. 2. (a) Electric voltage-induced change of the $H_{\rm eff}^{\rm OP}$, i.e., $\Delta H_{\rm eff}^{\rm OP}$, in the (001) Fe/BTO bilayers with various thicknesses d of the Fe(001) thin films. (b) Variation trends of $\Delta H_{\rm eff}^{\rm OP}$ as a function of the residual strain ε_0 in the (001) Fe/BTO bilayers at an applied voltage of 10 V.

In comparison with the Fe(001) film, the Ni(001) film presents different behavior, as shown in Fig. 3(a) for $\Delta H_{\rm eff}^{\rm OP}$ in the (001) Ni/BTO bilayer structure. A butterfly-shaped $\Delta H_{\rm eff}^{\rm OP}$-voltage curve is clearly shown even when the film thickness is reduced to 0.15 nm [see the inset of Fig. 3(a)], demonstrating the dominant influence of strain-mediated ME coupling in the (001) Ni/BTO heterostructure. Similarly to the (001) Fe/BTO case, the $\Delta H_{\rm eff}^{\rm OP}$-voltage curves reverse as the film thickness d exceeds the critical $d_{\rm cr}$ of about 1.76 nm (at $\varepsilon_0 = 2.5\%$[34]) and exhibit enhanced $\Delta H_{\rm eff}^{\rm OP}$ in the vicinity of $d_{\rm cr}$ where $H_{\rm eff}^{\rm OP}$ changes significantly. The (0001) Co/BTO structure also presents quite similar behavior [Fig. 3(b)], i.e., butterfly-shaped $\Delta H_{\rm eff}^{\rm OP}$-voltage behavior, demonstrating the dominant influence of strain-mediated ME coupling. Therefore, a significant interface-charge-mediated ME coupling may be difficult to be observed in such (001) Ni/BTO and (0001) Co/BTO bilayers wherein a robust strain-mediated ME coupling is always present in the case that the voltage-induced surface anisotropy change as shown in Fig. 1(b) is used for them. Meanwhile, the strain-induced $\Delta H_{\rm eff}^{\rm OP}$ in these two cases are much larger than that in the (001) Fe/BTO structure due to their larger magnetoelastic coupling coefficients.[36] Moreover, it should be noted that these butterfly-shaped $\Delta H_{\rm eff}^{\rm OP}$-voltage loops in the (001) Ni/ and (0001) Co/BTO bilayers exhibit opposite trends. This is due to the opposite signs of $H_{\rm eff}^{\rm OP}$ and different K_s[36] observed in the Ni(001) and Co(0001) films.

Now turn to an even more interesting FM/FE heterostructure consisting of an FM half-metal like LSMO. LSMO is used due to its high sensitivity of a strongly correlated magnetic state to the charge carriers.[19,20] In half-metals, the screening interface charges are usually 100% spin polarized, which in principle allows stronger ME coupling[43,44] as compared to the partial spontaneous spin polarization in FM metals such as Fe, Ni, and Co. For example, a universal surface ME constant of

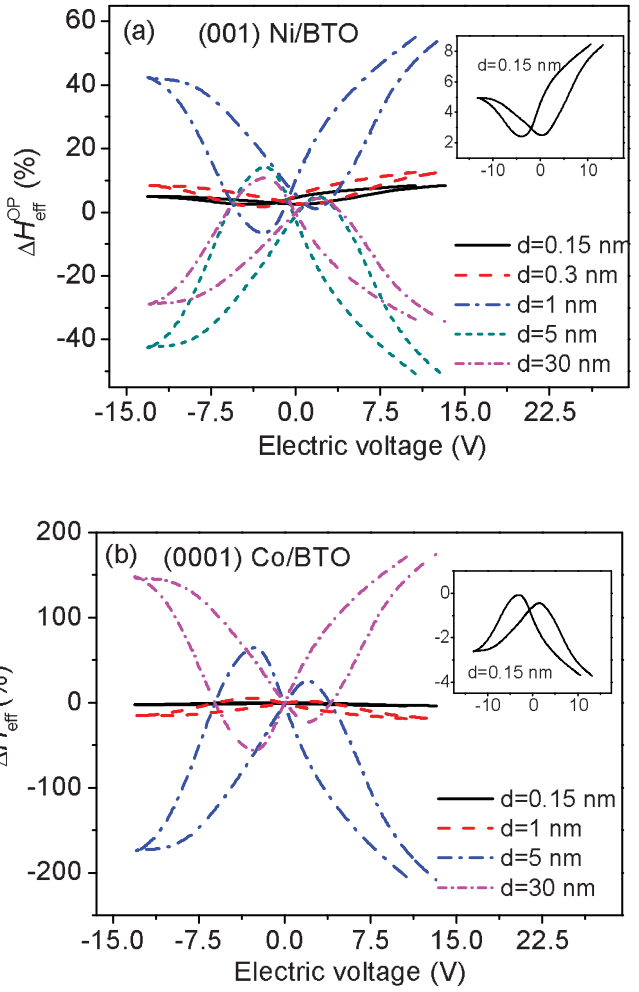

FIG. 3. Variations of the out-of-plane effective anisotropy field, i.e., $\Delta H_{\rm eff}^{\rm OP}$, with external electric voltages in (a) the (001) Ni/BTO and (b) the (0001) Co/BTO bilayers with different thicknesses d of the Ni or Co thin films.

about 6.44×10^{-14} G cm^2/V was derived for all FM half-metals,[44] which is about two to three times higher than that for FM metals, as mentioned above. Thus a larger voltage-induced surface anisotropy change is assumed for the half-metallic LSMO(001) films, as shown in Fig. 4(a). The sharp changes of ΔK_s in the vicinity of the FE coercive field can be related to the two distinct states for the spin-polarized interface charges resulting from the FE polarization reversal, i.e., the accumulation and the depletion state, respectively, as observed in a recent experiment.[19,20] Similarly to the case of the (001) Fe/BTO structure, the (001) LSMO/BTO heterostructure presents either hysteresis-like or butterfly-shaped $\Delta H_{\rm eff}^{\rm OP}$-voltage loops at room temperature [Fig. 4(b)], depending on the thickness of the LSMO films, exhibiting the interface-charge and strain co-mediated ME coupling. However, the room-temperature transition thickness $d_{\rm tr}$ in the (001) LSMO/BTO case is significantly larger than that in the (001) Fe/BTO case, i.e., about 4.2 nm, due to an enhanced ME coupling and thus the larger voltage-induced surface anisotropy change ΔK_s as discussed above. Furthermore, it can be seen that change in $\Delta H_{\rm eff}^{\rm OP}$ is greater in LSMO films with thickness above $d_{\rm tr}$ than that in LSMO thin films, indicating the voltage-controlled

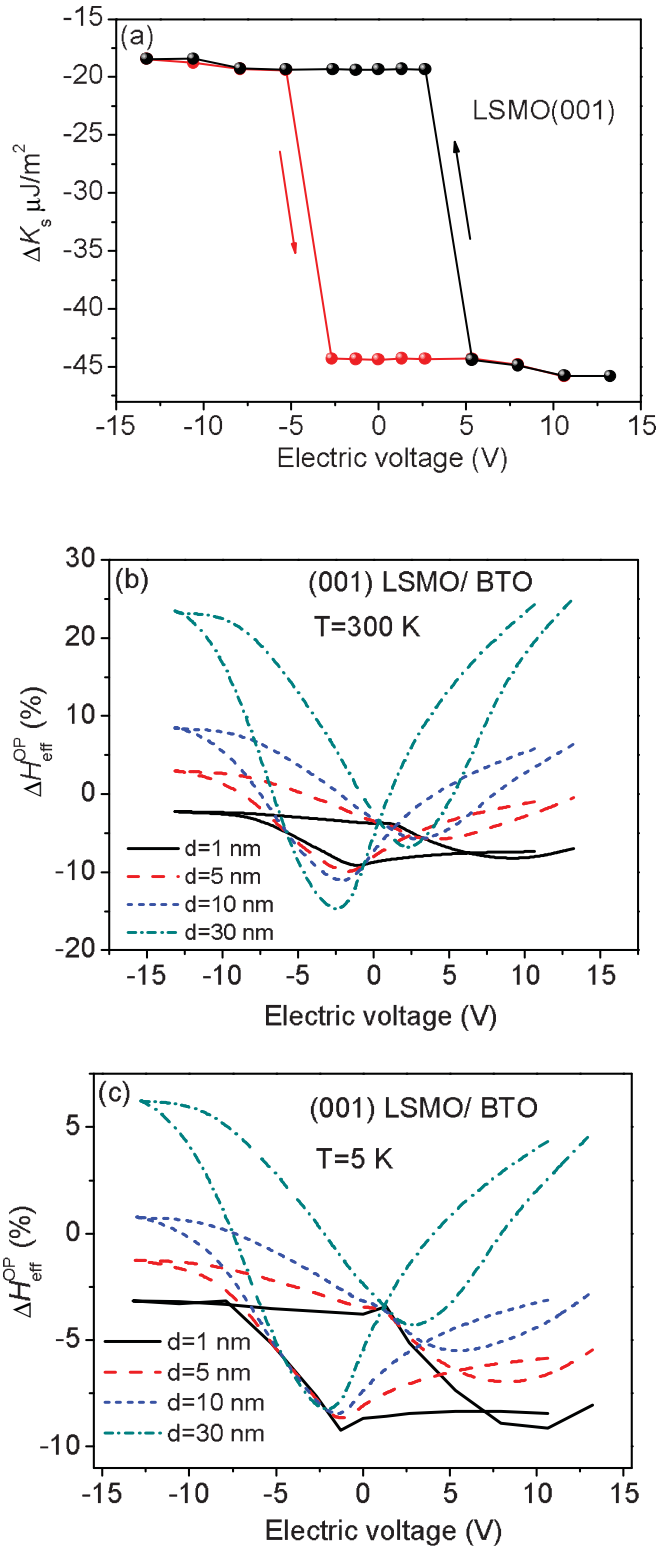

FIG. 4. (a) Electric voltage dependence of the surface anisotropy energy change ΔK_s in the (001)-oriented $La_{0.88}Sr_{0.1}MnO_3$ (LSMO) film. Electric voltage-induced change of the $H_{\rm eff}^{\rm OP}$, i.e., $\Delta H_{\rm eff}^{\rm OP}$, in the (001) LSMO/BTO bilayers with different thicknesses d of the LSMO thin films, at (b) T = 300 K and (c) T = 5 K.

magnetic anisotropy change may be more significant in the thick LSMO(001) films where the strain-mediated ME coupling dominates, as observed in recent experiments.[12,19,20]

The $\Delta H_{\text{eff}}^{\text{OP}}$-voltage curves of the LSMO/BTO structure at low temperature present a similar size-dependent behavior [Fig. 4(c)] to its room temperature case. However, it can be expected that the interface-charge-mediated ME effect would become more remarkable at low temperature in comparison with the suppressed strain-mediated ME coupling due to reduced piezoelectric strains, which can further lead to a larger transition thickness d_{tr}, demonstrating a major influence of the interface-charge-mediated ME coupling within a wider thickness range.

IV. CONCLUSIONS

In conclusion, a simple phenomenological model is able to describe the size-dependent electric voltage-controlled magnetic anisotropy in multiferroic heterostructures. The interface-charge- and strain-mediated coupling coexist and interact with each other in bilayer structures. A transition thickness d_{tr} is defined to describe the competition between these two coupling mechanisms, below which the influence of the interface-charge-mediated ME coupling would outweigh that of the strain-mediated ME coupling. The calculations show that interface-charge and strain co-mediated ME coupling can be clearly observed in the (001) Fe/BTO and the (001) LSMO/BTO structures. In particular, LSMO(001) films exhibit large transition thicknesses d_{tr}, indicating a more remarkable interface-charge-mediated ME effect. While in the (001) Ni/BTO and (0001) Co/BTO bilayers, the strain-mediated ME coupling could be always dominant, providing that they exhibit the same voltage-induced surface anisotropy contribution as in the (001) Fe.

ACKNOWLEDGMENTS

This work was supported by the NSF of China (Grant Nos. 50832003 and 50921061) and the National Basic Research Program of China (Grant No. 2009CB623303); and NSF under Grant No. DMR-1006541.

*Corresponding author: cwnan@tsinghua.edu.cn

[1] R. Ramesh and N. A. Spaldin, Nat. Mater. **6**, 348 (2007).
[2] Y. Wang, J.-M. Hu, Y. H. Lin, and C. W. Nan, NPG Asia Mater. **2**, 61 (2010).
[3] C. A. F. Vaz, J. Hoffman, C. H. Ahn, and R. Ramesh, Adv. Mater. **22**, 2900 (2010).
[4] C.-W. Nan, G. Liu, Y. Lin, and H. Chen, Phys. Rev. Lett. **94**, 197203 (2005).
[5] W. Eerenstein, N. D. Mathur, and J. F. Scott, Nature **442**, 759 (2006).
[6] M. Bibes and A. Barthélémy, Nat. Mater. **7**, 425 (2008).
[7] J.-M. Hu, Z. Li, J. Wang, and C. W. Nan, J. Appl. Phys. **107**, 093912 (2010).
[8] J.-M. Hu, Z. Li, J. Wang, J. Ma, Y. H. Lin, and C. W. Nan, J. Appl. Phys. **108**, 043909 (2010).
[9] J.-M. Hu, Z. Li, Y. H. Lin, and C. W. Nan, Phys. Status Solidi RRL **4**, 106 (2010).
[10] M. Liu, O. Obi, J. Lou, Y. J. Chen, Z. H. Cai, S. Stoute, M. Espanol, M. Lew, X. Situ, K. S. Ziemer, V. G. Harris, and N. X. Sun, Adv. Funct. Mater. **19**, 1826 (2009).
[11] M. Liu, O. Obi, Z. Cai, J. Lou, G. Yang, K. S. Ziemer, and N. X. Sun, J. Appl. Phys. **107**, 073916 (2010)
[12] C. Thiele, K. Dorr, O. Bilani, J. Rodel, and L. Schultz, Phys. Rev. B **75**, 054408 (2007).
[13] W. Eerenstein, M. Wiora, J. L. Prieto, J. F. Scott, and N. D. Mathur, Nat. Mater. **6**, 348 (2007).
[14] S. Sahoo, S. Polisetty, C.-G. Duan, S. S. Jaswal, E. Y. Tsymbal, and C. Binek, Phys. Rev. B **76**, 092108 (2007).
[15] J. J. Yang, Y. G. Zhao, H. F. Tian, L. B. Luo, H. Y. Zhang, Y. J. He, and H. S. Luo, Appl. Phys. Lett. **94**, 212504 (2009).
[16] J. Lou, M. Liu, D. Reed, Y. H. Ren, and N. X. Sun, Adv. Mater. **21**, 4711 (2009).
[17] S. Geprags, A. Brandlmaier, M. Opel, R. Gross, and S. T. B. Goennenwein, Appl. Phys. Lett. **96**, 142509 (2010).
[18] J.-M. Hu and C. W. Nan, Phys. Rev. B **80**, 224416 (2009).
[19] H. J. A. Molegraaf, J. Hoffman, C. A. F. Vaz, S. Gariglio, D. van der Marel, C. H. Ahn, and J. M. Triscone, Adv. Mater. **21**, 3470 (2009).
[20] C. A. F. Vaz, J. Hoffman, Y. Segal, J. W. Reiner, R. D. Grober, Z. Zhang, C. H. Ahn, and F. J. Walker, Phys. Rev. Lett. **104**, 127202 (2010).
[21] M. Weisheit, Science **315**, 349 (2007).
[22] T. Maruyama, Y. Shiota, T. Nozaki, K. Ohta, N. Toda, M. Mizuguchi, A. A. Tulapurkar, T. Shinjo, M. Shiraishi, S. Mizukami, Y. Ando, and Y. Suzuki, Nat. Nanotech. **4**, 158 (2009).
[23] M. Endo, S. Kanai, S. Ikeda, F. Matsukura, and H. Ohno, Appl. Phys. Lett. **96**, 212503 (2010).
[24] P. Borisov, A. Hochstrat, X. Chen, W. Kleemann, and C. Binek, Phys. Rev. Lett. **94**, 117203 (2005).
[25] V. Laukhin, V. Skumryev, X. Martí, D. Hrabovsky, F. Sánchez, M. V. García-Cuenca, C. Ferrater, M. Varela, U. Lüders, J. F. Bobo, and J. Fontcuberta, Phys. Rev. Lett. **97**, 227201 (2006).
[26] Y. H. Chu, L. W. Martin, M. B. Holcomb, M. Gajek, S. J. Han, Q. He, N. Balke, C. H. Yang, D. Lee, W. Hu, Q. Zhan, P. L. Yang, A. Fraile-Rodriguez, A. Scholl, S. X. Wang, and R. Ramesh, Nat. Mater. **7**, 478 (2008).
[27] H. Béa, M. Bibes, F. Ott, B. Dupé, X. H. Zhu, S. Petit, S. Fusil, C. Deranlot, K. Bouzehouane, and A. Barthélémy, Phys. Rev. Lett. **100**, 017204 (2008).
[28] D. Lebeugle, A. Mougin, M. Viret, D. Colson, and L. Ranno, Phys. Rev. Lett. **103**, 257601 (2009).
[29] D. Lebeugle, A. Mougin, M. Viret, D. Colson, J. Allibe, H. Béa, E. Jacquet, C. Deranlot, M. Bibes, and A. Barthélémy, Phys. Rev. B **81**, 134411 (2010).
[30] D. Peterka, A. Enders, G. Haas, and K. Kern, Phys. Rev. B **66**, 104411 (2002).
[31] J. X. Zhang, Y. L. Li, D. G. Schlom, L. Q. Chen, F. Zavaliche, R. Ramesh, and Q. X. Jia, Appl. Phys. Lett. **90**, 052909 (2007).
[32] J. Lou, R. E. Insignares, Z. Cai, K. S. Ziemer, M. Liu, and N. X. Sun, Appl. Phys. Lett. **91**, 182504 (2007).

[33]R. C. O' Handley, O. S. Song, and C. A. Ballentine, J. Appl. Phys. **74**, 6302 (1993).

[34]R. Vollmer, Th. Gutjahr-Löser, J. Kirschner, S. van Dijken, and B. Poelsema, Phys. Rev. B **60**, 6277 (1999).

[35]A. Stupakiewicz, A. Maziewski, K. Matlak, N. Spiridis, M. Slezak, T. Slezak, M. Zajkac, and J. Korecki, Phys. Rev. Lett. **101**, 217202 (2008).

[36]The parameters used for numerical calculations are as follows. For Fe, $c_{11} = 229$ GPa, $c_{12} = 134$ GPa, $K_1 = 0.048$ MJ/m^3, $K_2 = 0.0001$ MJ/m^3, $B_1 = -3.43$ MJ/m^3, $M_s = 1.7 \times 10^6$ A/m (Ref. 18), $K_s = 0.29$ mJ/m^2 (Ref. 22); for Ni, $c_{11} = 246.5$ GPa, $c_{12} = 147.3$ GPa, $K_1 = -0.0045$ MJ/m^3, $K_2 = -0.0023$ MJ/m^3, $B_1 = 9.2$ MJ/m^3, $M_s = 4.85 \times 10^5$ A/m (Ref. 18), $K_s = -0.31$ mJ/m^2 (Ref. 34); for $La_{0.88}Sr_{0.1}MnO_3$, $c_{11} = 200$ GPa, $c_{12} = 105$ GPa, $K_1 = 0.127$ MJ/m^3, $K_2 = -0.174$ MJ/m^3, $K_s = 0.5$ mJ/m^2, $B_1 = -1.43$ MJ/m^3, $M_s = 3 \times 10^5$ A/m (Refs. 37–39); for hexagonal Co, $c_{11} = 307$ GPa, $c_{12} = 165$ GPa, $c_{13} = 103$ GPa, $c_{33} = 358$ GPa, $c_{44} = 75.5$ Gpa, $K_1 = 0.513$ MJ/m^3, $K_2 = 0.013$ MJ/m^3, $B_1 = -8.1$ MJ/m^3, $B_2 = -29$ MJ/m^3, $B_3 = 28.2$ MJ/m^3, $B_4 = 29.4$ MJ/m^3, $M_s = 1.45 \times 10^6$ A/m (Ref. 40), $K_s = 1.16$ mJ/m^2 (Ref. 35).

[37]Z.-H. Wang, H. Kronmüller, O. I. Lebedev, G. M. Gross, F. S. Razavi, H. U. Habermeier, and B. G. Shen, Phys. Rev. B **65**, 054411 (2002).

[38]Y. F. Popov, A. M. Kadomtseva, G. P. Vorob'ev, V. Y. Ivanov, A. A. Mukhin, A. K. Zvezdin, and A. M. Balbashov, J. Appl. Phys. **83**, 7160 (1998).

[39]J. O'Donnell, M. S. Rzchowski, J. N. Eckstein, and I. Bozovic, Appl. Phys. Lett. **72**, 1775 (1998).

[40]D. Sander, A. Enders, and J. Kirschner, J. Magn. Magn. Mater. **200**, 439 (1999).

[41]Y. Zhang, J. Liu, X. H. Xiao, T. C. Peng, C. Z. Jiang, Y. H. Lin, and C. W. Nan, J. Phys. D: Appl. Phys. **43**, 082002 (2010).

[42]C.-G. Duan, J. P. Velev, R. F. Sabirianov, Z. Zhu, J. Chu, S. S. Jaswal, and E. Y. Tsymbal, Phys. Rev. Lett. **101**, 137201 (2008).

[43]T. Y. Cai, S. Ju, J. Lee, N. Sai, A. A. Demkov, Q. Niu, Z. Li, J. Shi, and E. G. Wang, Phys. Rev. B **80**, 140415 (2009).

[44]C.-G. Duan, C.-W. Nan, S. S. Jaswal, and E. Y. Tsymbal, Phys. Rev. B **79**, 140403 (2009).